

# PROCEEDINGS OF SPIE

SPIEDigitalLibrary.org/conference-proceedings-of-spie

## Tunable, angle and polarization-insensitive broadband absorber

Jiang, Xinpeng, Yang, Junbo, Zhang, Zhaojian, Zhang, Jingjing, Xie, Wanlin

Xinpeng Jiang, Junbo Yang, Zhaojian Zhang, Jingjing Zhang, Wanlin Xie,  
"Tunable, angle and polarization-insensitive broadband absorber," Proc. SPIE  
11440, 2019 International Conference on Optical Instruments and Technology:  
Micro/Nano Photonics: Materials and Devices, 114400E (12 March 2020); doi:  
10.1117/12.2547546

**SPIE.**

Event: 2019 International Conference on Optical Instruments and Technology,  
2019, Beijing, China

# Tunable, angle and polarization-insensitive broadband absorber

XINPENG JIANG<sup>\*a</sup>, JUNBO YANG<sup>b</sup>, ZHAOJIAN ZHANG<sup>a</sup>, JINGJING ZHANG<sup>a</sup>, WANLIN XIE<sup>a</sup>

<sup>a</sup>College of Liberal Arts and Sciences, National University of Defense Technology, Changsha 410073, China; <sup>b</sup>Center of Material Science, National University of Defense Technology, Changsha 410073, China; \*Comtact Author: jackson97666@163.com

## ABSTRACT

Using the principle of Surface Plasmons Polaritons, we propose a graphene broadband terahertz absorption structure that achieves the tunable absorption of electromagnetic waves. In our absorption structure, the method of patterning graphene is used to realize continuous broadband absorption from 0.5THz to 2.1THz. The absorption which is more than 50% reaches 1.1THZ, especially the structure designed here has three plasmonic resonance peaks which above 98% at 0.79THz, 1.18THz and 1.35THz, respectively. In addition, the symmetry in the pattern design consider that our absorption structure is not sensitive to the polarization and incident angle. Due to a series of excellent characteristics of the absorption structure, it may play an important role in the field of aircraft stealth, absorber, and light wave modulation.

**Keywords:** Surface Plasmons Polaritons, metamaterial, Graphene absorber, Terahertz, Continuous broadband

## 1. INTRODUCTION

Begin the Introduction two lines below the Keywords. The manuscript should not have headers, footers, or page numbers. It should be in a one-column format. References are often noted in the text<sup>1</sup> and cited at the end of the paper. As a new two-dimensional material, graphene has received wide attention in recent years due to many specific properties, such as quantum electron transport<sup>[1-4]</sup>, adjustable band gap<sup>[5]</sup>, extremely high mobility, electromechanical modulation and so on. In the terahertz band, graphene can excite Surface Plasmons Polaritons(SPP) which play a significant role in design of adsorber. Through the metamaterial structure pattern design, we can achieve a wider range of electromagnetic properties than continuous graphene. Thus, the structured graphene metamaterial may finally produce functional devices such as: detector<sup>[6]</sup>, sensor<sup>[7]</sup>, modulator<sup>[8]</sup> and optical stealth<sup>[9,10]</sup>. In this paper we will focus on the role of graphene in designing absorber structures.

Graphene is an optically transparent material that has an absorption rate of only 2.3% per layer in the optical range, but it has a high absorption characteristic in the terahertz band. Using the principle of SPP and some techniques can achieve nearly 100% perfect absorption in a specific wavelength band. Despite this, most of the absorbing structures can only achieve perfect absorption of the narrow band. After the patterning process, we use a simple pattern to achieve a perfect absorption of a wide spectral range.

In this paper, we propose a tunable, angle and polarization-insensitive broadband absorber based on SPP. Our structure is a sandwich structure, which consists of the patterned graphene, ideally mirrored, separated by silica between the mirror layer and the graphene. The superposition coupling between the graphene rings allows our device to significantly expand the operating bandwidth of the device under certain conditions. At the same time, because of the perfect symmetry of the graphene ring geometry, the function of our device is insensitive to the angle and the polarization. Finally, thanks to the tunability of the Fermi energy of graphene, we can effectively modulate the operating band of the device by modulating the Fermi energy of the graphene layer. Our results may offer new possibilities for SPP and metamaterials to be applied to terahertz bands and other bands to implement tunable devices.

## 2. RESULT AND DISCUSSION

### 2.1 Graphene conductivity tunability principle

In the proposed study, it is theoretically possible to calculate the conductivity value  $\sigma$  using the Kubo formula [11], taking into account the in-band and inter-band transitions by the formula [12-14]

$$\begin{aligned}\sigma_{gra} = \sigma_{int\ ra} + \sigma_{inter} &= \frac{2e^2k_B T}{\pi\hbar^2} \frac{i}{\omega+i/\tau} \ln \left[ 2 \cosh \left( \frac{E_f}{2k_B T} \right) \right] \\ &+ \frac{e^2}{4\hbar^2} \left[ \frac{1}{2} + \frac{1}{\pi} \arctan \left( \frac{\hbar\omega - 2E_f}{2k_B T} \right) - \frac{i}{2\pi} \ln \frac{(\hbar\omega + 2E_f)^2}{(\hbar\omega - 2E_f)^2 + 4(k_B T)^2} \right]\end{aligned}\quad (1)$$

Where  $\omega$  is the angular frequency,  $E_f$  is the Fermi level,  $\tau$  is the electron-phonon relaxation time, and  $T$  is the ambient temperature. Also,  $k_B$ ,  $e$ , and  $\hbar$  are the Boltzman constant, the electron charge and the Plank constant, respectively. For the THz frequency domain at room temperature, the interband transitions are negligibly small according to the Pauli exclusion principle, so the surface conductivity can be safely reduced to a class of Drude models [15-17].

$$\sigma_{gra} = \frac{e^2 E_f}{\pi\hbar^2} \frac{i}{(\omega+i/\tau)} \quad (2)$$

The principle of graphene conductivity tunability provides the possibility to modulate the work bandwidth of the device, and its Fermi energy can be freely adjusted over a wide range by applying an electrostatic bias [11].

### 2.2 Double loop system performance test

First, we tested the performance of the graphene concentric double ring system (GCDRS). Due to the SPP of the graphene, we can know that a single graphene ring can generate absorption peaks for a specific band. After program simulation, we also verify that it can be single. The graphene ring will produce a specific strong absorption in a certain band. With this absorption characteristic, we try to connect the absorption peaks of two relatively close bands by the nesting of the GCDRS to improve the absorption structure of the work bandwidth.

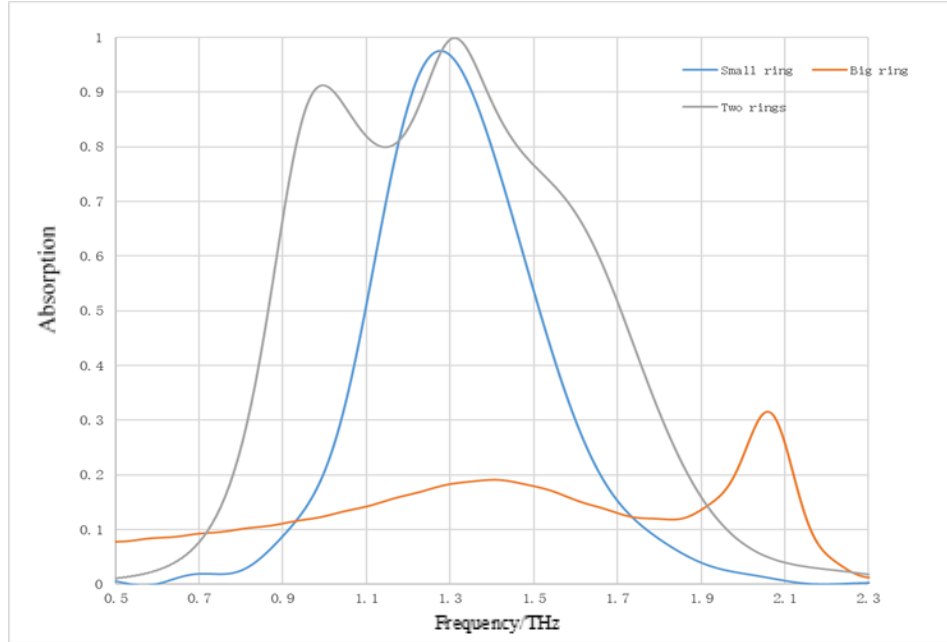


Figure 1. Simulated absorption spectra of the proposed GCDR absorber (grey line) and two graphene single ring absorbers with the top graphene double ring replaced by the isolated inner ring (red line) and outer ring (blue line).

The absorption bandwidth and efficiency of the perfect absorber are greatly improved compared with the previous one. As a trigger, we try to couple the third ring with this structure, in order to achieve a larger absorption bandwidth.

### 2.3 Simulation of three-ring system

From the SPP of graphene and the test of the GCDRS, it can be known that the change of the size of the graphene pattern can make the absorber produce specific absorption for electromagnetic waves of different wavelength bands. Compared with the double-loop system, through repeated tests, we use the graphene concentric three rings system (GCTRS) to achieve a wider absorption bandwidth than the double ring. And then we find that the absorption peak in a specific band also appears blue shift or red shift which is very beneficial for only enough ring nesting.

Now we will specifically describe our absorber and give the simulation data for your reference. Figure 2 depicts a schematic of the proposed metamaterial-based perfect absorber (MPA) consisting of a single layer of three graphene structure arrays and an optical thick gold mirror separated by a  $28\mu\text{m}$  thick lossless  $\text{SiO}_2$  spacer, where  $\varepsilon_d = 3.9$ . Here, the inner and outer graphene rings of the concentric rings are optimized with  $1.5\mu\text{m}$  separation to induce superposition effects to achieve the desired broadband absorption (see detailed structural parameters in the header of Figure 2). In addition, the use of a metal ground plane will ensure complete reflection of the impact terahertz wave, just like a "mirror". In our proposed device, a layer of ion-gel was spin-coated on the graphene pattern and contacted with the Au electrode as a top gate. At the same time, an ultra-thin transparent conductive thin layer<sup>[18]</sup> is deposited between the  $\text{SiO}_2$  layer and the graphene ring as the bottom gate.

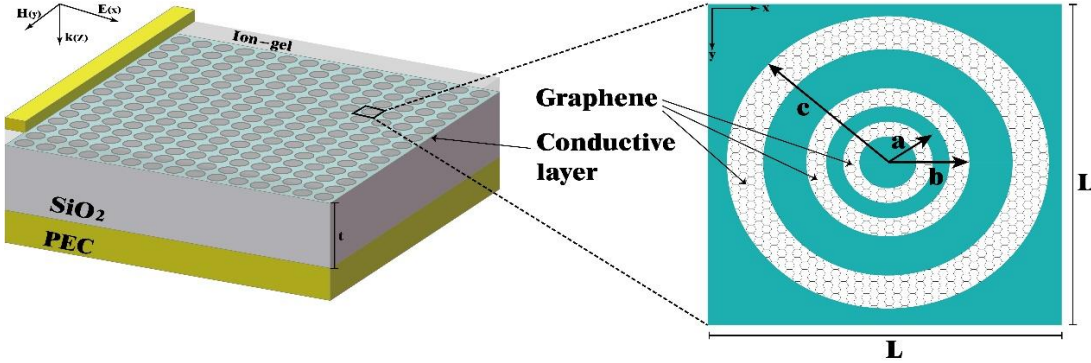


Figure 2. Schematic illustration of a broadband THz absorber consisting of three-ring graphene absorber structures and an ideal conductor mirror separated by a thin  $\text{SiO}_2$  spacer. The ion-gel was spin coated onto the graphene nanostructures and contacted with an Au electrode as a top gate. And an ultra-thin and transparent conductive thin layer is deposited as a bottom gate between  $\text{SiO}_2$  and graphene. The geometrical parameters of the three-layer graphene are  $a=2.5\mu\text{m}$ ,  $b=5.5\mu\text{m}$ ,  $c=10\mu\text{m}$ ,  $t=28\mu\text{m}$ , the boundary of a periodic unit is  $L=28\mu\text{m}$ .

In our study, we chose an initial value of  $E_f=0.5\text{eV}$  and then test its value to study the proposed function of graphene MPA. For the sake of simplicity, we chose a fixed relaxation time of  $\tau=1\text{ps}$  (corresponding to electron mobility), which is large but achievable for high quality graphene obtained by mechanical stripping<sup>[19, 20]</sup>. Strictly speaking, Fermi energy and the frequency<sup>[21]</sup> determine the relaxation time of graphene. However, this set of effects is usually weak, so they do not affect the main conclusions of this paper.

The working principle of this reflective MPA can be understood as follows. When the electromagnetic wave illuminates the device, the SPP is excited on the top graphene layer and the redundant energy which wastages in the absorber was reflect by the bottom metal mirror, resulting in strong magnetic resonance<sup>[22-25]</sup>. It is known from the properties of SPP that the SPP excited by the MPA will change the direction of energy propagation, thereby achieving the loss of these energy at the surface without reflection. In the works<sup>[18, 26-28]</sup> done by the predecessors, a local surface plasma mode or a gap plasma mode illuminated by incident light will be excited inside the graphene microstructure, resulting in a significant enhancement of light absorption.

We tested the absorption of our graphene absorption structure. Of course, if we change the Fermi level of the absorption structure, then from the above principle about the adjustability of graphene conductivity, we can change the absorption band of the absorption structure, thus reflecting The tunability of our structure. Below we will show our absorption spectrum by taking the graphene structure of Fermi level  $E_f=0.5\text{eV}$  as an example.

First, we placed an X-polarized THz wave into the MPA with three ring-shaped graphene patterns, as shown in Figure 2. The calculated absorption spectrum of the proposed graphene MPA (see red line) was depicted in Figure 3 (a), the top view of which is shown in Figure 3 (c). It is worth noting that the proposed device exhibits a high absorption rate of more than 70% from 0.74 to 1.69 THz. Moreover, there are three absorption peaks at about 0.8THz, 1.12THz, and 1.26THz in the frequency band. To clarify their physical origin, we further calculated the absorption spectra of two simplified graphene surfaces, the original three-layer periodic graphene structure of the top layer being isolated by the inner ring and the ring sandwiched between them (see Figure 3 (d)) and the isolated outer ring is replaced (see Figure 3(a)). Obviously, when the incident wave is incident on the absorbing structure shown in Fig. 3(d) (top view), the formant appears at about 0.98THz and 1.30THz (see the gray line in Fig. 3(a)), which should correspond to The last two

absorption peaks of the three-layer periodic graphene structure (see the red line in Figure 3(a)). Similarly, the absorption peak at 0.77THz of the absorber consisting of the outer graphene ring (see the blue line in Figure 3(a)) should correspond to the low-frequency absorption peak of the three-layer periodic graphene structure (see Figure 3 (see Figure 3). a) gray line). Interestingly, although the three graphene single-ring (GSR) surfaces exhibit limited absorption and narrow bandwidth, the three-layer periodic graphene structure absorber can be used as a perfect THz absorber with high absorption rate which is more than 70% from 0.74THz to 1.69THz. In addition, compared to the three-layer periodic graphene structure absorber compared, the low frequency peak was red shifted from 1.30THz to 1.26THz, the high frequency peak was shifted from 0.77THz blue to 0.8THz. Therefore, the three-layer periodic graphene structure absorber can work well in a larger frequency band. In fact, we use the coupling effect between the three GSRs, on the one hand, to prove that the finite increase of the microstructure of the absorbing structure can significantly improve the absorbing efficiency, and the superposition of a finite number of absorbing structures will produce “1+1”. The effect of more than 2”, on the other hand, also proves that not only the effect of orbital hybridization of the two-cycle graphene structure exists, but also exists in the three-cycle graphene structure, and with this method we can produce more absorption efficiency and wider absorption band absorbing structure to achieve good performance of the proposed GCDR absorber [28-30].

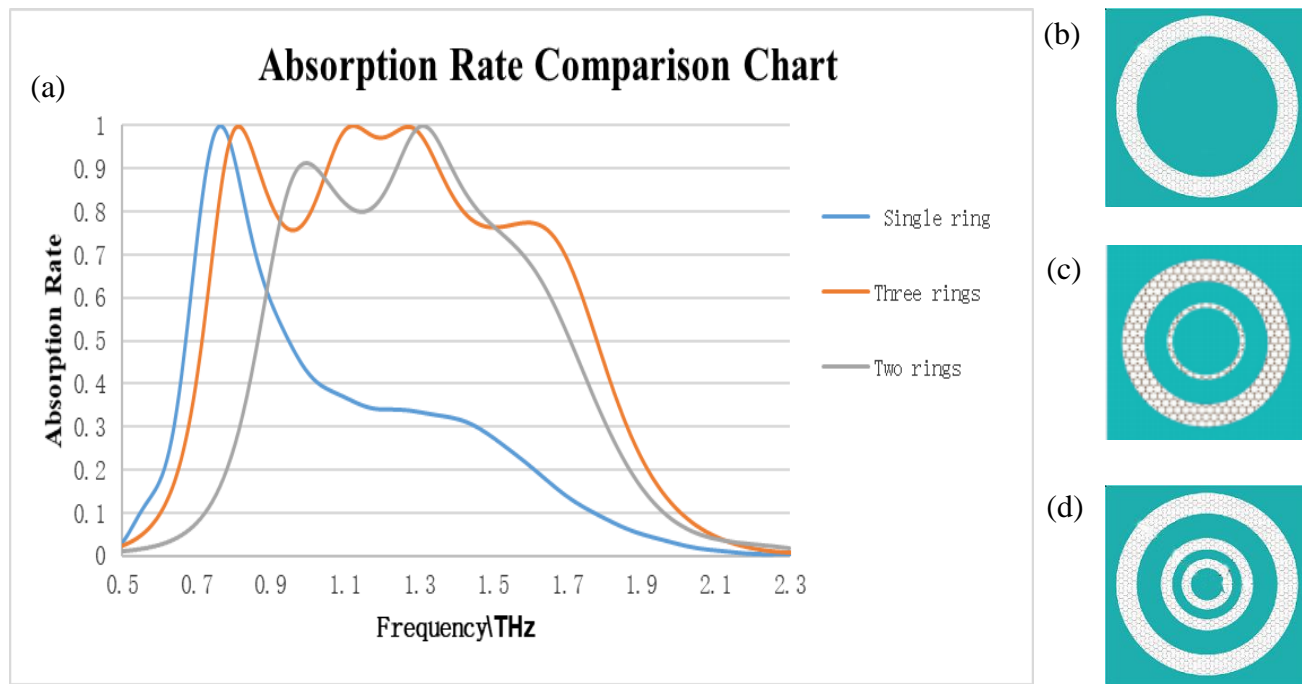


Figure 3. (a-d) (a) Simulated absorption spectra of the proposed graphene concentric three rings absorber (red line) and GCDR absorber (grey line) and a GSR absorber with the top graphene ring replaced by the isolated outer ring (blue line). (b-d) Top views of three graphene MPAs comprised by the single outer ring, double rings and three rings, respectively.

Next, we performed a full wave simulation to verify the superposition coupled model used in the proposed graphene absorber structure. And we gave an analysis of the red-blue shift of the absorption peak of the three-ring system compared to the two-ring system. We selected images with frequencies at three absorption peak positions to observe the superposition of the absorption structure. From Fig. 4 (a), we can see that there is a coupling effect between the outer ring and the intermediate ring at 0.8THz, which is also an important reason for the blue shift of the first absorption peak. From Fig. 4 (b), we can see that the coupling effect of the inner ring and the intermediate ring is obvious in the case of 1.12THz, which also provides a basis for our second absorption peak blue shift. Although the coupling of the outer ring in the system also affects the movement of the absorption peak, it does not play a decisive role in the movement of the second absorption peak. Of course, the effect of the outer ring on the overall absorption rate is significant. We can see from Fig.3 (a) (see the red line) that the interposition of the outer ring causes a significant increase in the intermediate absorption peak, which is for the absorption structure. It can be seen from Fig. 4 (c) that the inner ring and the

intermediate ring have a good coupling, which in turn causes a red shift in the last absorption peak. Through full-wave analysis, on the one hand, we see that the coupling of the three rings is indeed interlocking and selective. And this coupling and selectivity are highly dependent on the distance of the different rings and the size of each ring. On the other hand, we also explained the reasons for the red shift and blue shift of the absorption peak by full-wave analysis. In particular, through full-wave analysis, we found the basis for the blue shift of the intermediate peak instead of the red shift, which also reflects the authenticity and reliability of our simulation from one side.

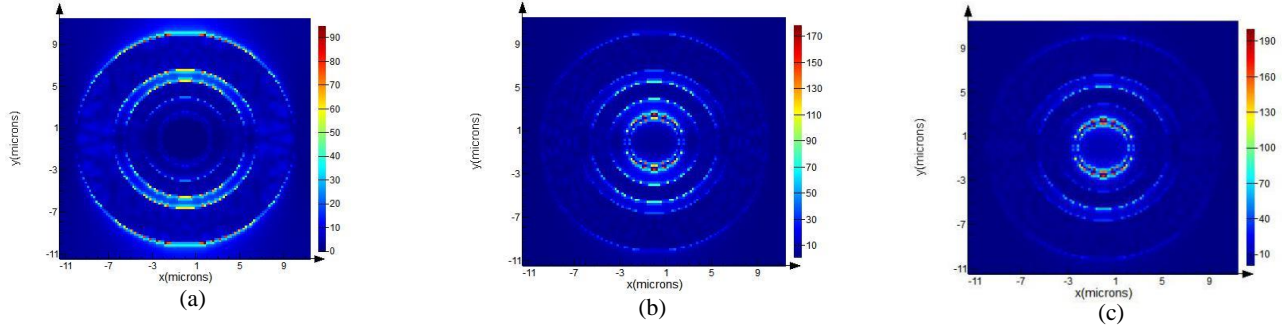


Figure 4. (a-c) The simulated electric field pattern at the top graphene layer of the absorbing structure shown in is at a corresponding absorption peak (a) of 0.8 THz, (b) is 1.12 THz, and (c) is 1.26 THz.

#### 2.4 The discussion of the angle and polarization insensitivity

The polarization angle dependence of the graphene absorption structure was proposed by our institute. Figures 5 (a) and (b) respectively depict the angular relationship of the polarized light field incident on the absorber and the relationship of the polarization angle  $\varphi$  with respect to the absorber. Obviously, because of the perfect ring structure which the graphene pattern is, the absorption rate of our device is strictly unchanged from the polarization angle  $\varphi$ . The perfect symmetry of this structure will inevitably cause our absorber to be insensitive to the change of polarization angle. As the polarization angle changes, the SPP generated by the terahertz wave incident on the absorber can be excited all the way inside the structure, except that their orientation angles simultaneously rotate with the incident electric field.

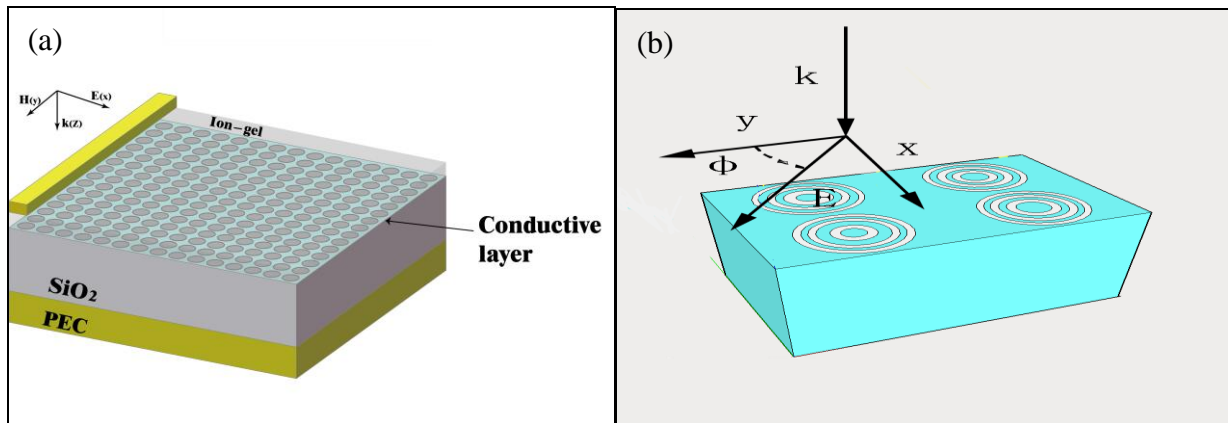


Figure 5. (a-b). (a) The case that X-polarized THz waves are normally illuminated on the device. (b) Absorption characteristics of the proposed absorber for normally incident waves with different polarization angle  $\varphi$

### 3. CONCLUSION

In summary, we proposed tunable, angle and polarization-insensitive broadband absorber based on graphene Surface Plasmons Polaritons. The multilayer graphene structure helps us to expand the absorption of the sandwich structure, thereby achieving broadband absorption. Compared to conventional metamaterial absorbers, graphene-based devices can achieve a smaller size. And using the pattern design method we have achieved a wider absorption range than the previous structure, we believe that the use of this pattern design can further design a more sophisticated and sensitive wide band absorber.

### ACKNOWLEDGEMENTS

This work is supported by the National Natural Science Foundation of China (60907003, 61805278), the China Postdoctoral Science Foundation (2018M633704), the Foundation of NUDT (JC13-02-13, ZK17-03-01), the Hunan Provincial Natural Science Foundation of China (13JJ3001), and the Program for New Century Excellent Talents in University (NCET-12-0142).

### REFERENCES

- [1] K. S. Novoselov, A. K. Geim, S. V. Morozov, D. Jiang, M. I. Katsnelson, I. V. Grigorieva, S. V. Dubonos, and A. A. Firsov, *Nature* 438, 197 (2005).
- [2] Z. Jiang, E. A. Henriksen, L. C. Tung, Y.-J. Wang, M. E. Schwartz, M. Y. Han, P. Kim, and H. L. Stormer, *Phys. Rev. Lett.* 98, 197403 (2007).
- [3] R. S. Deacon, K.-C. Chuang, R. J. Nicholas, K. S. Novoselov, and A. K. Geim, *Phys. Rev. B* 76, 081406 (2007).
- [4] Z. Li, E. A. Henriksen, Z. Jiang, Z. Hao, M. C. Martin, P. Kim, H. L. Stormer, and D. N. Basov, *Nature Physics* 4, 532 (2008).
- [5] K. Aydin, V. E. Ferry, R. M. Briggs, and H. A. Atwater, “Broadband polarization-independent resonant light absorption using ultrathin plasmonic super absorbers,” *Nat. Commun.* 2, 517 (2011).
- [6] Wang, J., Gou, J. & Li, W. Preparation of room temperature terahertz detector with lithium tantalate crystal and thin film. *Aip Advances* 4, 97–105 (2014).
- [7] Yahiaoui, R. et al. Multispectral terahertz sensing with highly flexible ultrathin metamaterial absorber. *Journal of Applied Physics* 118, 083103 (2015).
- [8] Savo, S., Shrekenhamer, D. & Padilla, W. J. Liquid crystal metamaterial absorber spatial light modulator for THz applications. *Advanced Optical Materials* 2, 275–279 (2014).
- [9] J. B. Pendry, D. Schurig, and D. R. Smith, “Controlling electromagnetic fields,” *Science* 312(5781), 1780–1782 (2006).
- [10] U. Leonhardt, “Optical Conformal Mapping,” *Science* 312(5781), 1777–1780 (2006)
- [11] V. P. Gusynin, S. G. Sharapov, and J. P. Carbotte, *J. Phys. Condens. Mat.* 19, 026222 (2007).
- [12] U. Leonhardt, “Optical Conformal Mapping,” *Science* 312(5781), 1777–1780 (2006).
- [13] N. I. Landy, S. Sajuyigbe, J. J. Mock, D. R. Smith, and W. J. Padilla, “Perfect Metamaterial Absorber,” *Phys. Rev. Lett.* 100(20), 207402 (2008).
- [14] T. V. Teperik, F. J. Garc á de Abajo, A. G. Borisov, M. Abdelsalam, P. N. Bartlett, Y. Sugawara, and J. J. Baumberg, “Omnidirectional absorption in nanostructured metal surfaces,” *Nat. Photonics* 2(5), 299–301 (2008).
- [15] S.J. Zinkle, K.A. Terrani, J.C. Gehin, L.J. Ott, L.L. Snead, Accident tolerant fuels for LWRs: a perspective, *J. Nucl. Mater.* 448 (2014).
- [16] N. Liu, M. Mesch, T. Weiss, M. Hentschel, and H. Giessen, “Infrared perfect absorber and its application as plasmonic sensor,” *Nano Lett.* 10(7), 2342–2348 (2010).
- [17] J. Hao, J. Wang, X. Liu, W. J. Padilla, L. Zhou, and M. Qiu, “High performance optical absorber based on a plasmonic metamaterial,” *Appl. Phys. Lett.* 96(25), 251104 (2010).
- [18] C.M. Parish, K.A. Unocic, L. Tan, S.J. Zinkle, S. Kondo, L.L. Snead, D.T. Hoelzer, Y. Katoh, Helium sequestration at nanoparticle-matrix interfaces in helium  $\beta$  heavy ion irradiated nanostructured ferritic alloys, *J. Nucl. Mater.* 483 (2017).

- [19] M. Hong, F. Ren, H. Zhang, X. Xiao, B. Yang, C. Tian, D. Fu, Y. Wang, C. Jiang, Enhanced radiation tolerance in nitride multilayered nanofilms with small period-thicknesses, *Appl. Phys. Lett.* 101 (2012).
- [20] H. Tao, N. I. Landy, C. M. Bingham, X. Zhang, R. D. Averitt, and W. J. Padilla, “A metamaterial absorber for the terahertz regime: design, fabrication and characterization,” *Opt. Express* 16(10), 7181–7188 (2008).
- [21] X. Shen, T. J. Cui, J. Zhao, H. F. Ma, W. X. Jiang, and H. Li, “Polarization-independent wide-angle triple-band metamaterial absorber,” *Opt. Express* 19(10), 9401–9407 (2011).
- [22] *J. Appl. Phys.* 114,234304 (2013). Copyright 2013 AIP Publishing LLC.
- [23] G. Ackland, Controlling radiation damage, *Science* 327 (2010).
- [24] M. Lei, N. Feng, Q. Wang, Y. Hao, S. Huang, and K. Bi, “Magnetically tunable metamaterial perfect absorber,” *J. Appl. Phys.* 119(24), 244504 (2016).
- [25] N. I. Landy, C. M. Bingham, T. Tyler, N. Jokerst, D. R. Smith, and W. J. Padilla, “Design, theory, and measurement of a polarization-insensitive absorber for terahertz imaging,” *Phys. Rev. B*79(12), 125104 (2009).
- [26] A. K. Geim and K. S. Novoselov, “The rise of graphene,” *Nat. Mater.* 6(3), 183–191 (2007).
- [27] R. Alaei, M. Farhat, C. Rockstuhl, and F. Lederer, “A perfect absorber made of a graphene micro-ribbon metamaterial,” *Opt. Express* 20(27), 28017–28024 (2012).
- [28] S. Thongrattanasiri, F. H. L. Koppens, and F. J. García de Abajo, “Complete optical absorption in periodically patterned graphene,” *Phys. Rev. Lett.* 108(4), 047401 (2012).
- [29] Y. Zhang, Y. Feng, B. Zhu, J. Zhao, and T. Jiang, “Graphene based tunable metamaterial absorber and polarization modulation in terahertz frequency,” *Opt. Express* 22(19), 22743–22752(2014).
- [30] Z. Fang, Y. Wang, A. E. Schlather, Z. Liu, P. M. Ajayan, F. J. Garc ía de Abajo, P. Nordlander, X. Zhu, and N. J. Halas, “Active tunable absorption enhancement with graphene nanodisk arrays,” *Nano Lett.* 14(1), 299–304 (2014).